Bioinspired Layered Composites Based on Flattened Double-Walled Carbon Nanotubes

Qunfeng Cheng, Mingzhu Li, Lei Jiang, and Zhiyong Tang**

Carbon nanotubes (CNTs) are receiving much attention in the field of composites due to their extremely high tensile strength of around 100 GPa and Young's modulus of around 1000 GPa.[1] Unfortunately, the mechanical properties of CNT-reinforced polymer composites are far lower than theory predicts; this is due to low volume fraction, possible phase separation, random orientation, and weak interfacial load transfer in CNT/polymer composites.[2] Recently, several methods have been developed to fabricate composites with high CNT loading of up to 60 wt%, including one-dimensional (1D) CNT/polymer fibers,[3] and three-dimensional (3D) bulk materials, such as buckypaper,[4] mechanical densification,[5] layer-by-layer (LBL) assembly,[6] prepregging process,[7] and resin transfer molding.[8] However, it still remains a significant technical challenge to fabricate high performance composites with high CNT loading and distinct structural features. As a successful example, the fantastic layered structure of natural nacre, in which the inorganic content (calcium carbonate) can reach up to almost 95 vol-% without phase separation, has superior mechanical performance.[9] Inspired by relationship of the structure and the mechanical strength in nacre, we suggest that CNT-reinforced polymer composites having a layered structure may have excellent mechanical performance.

In this work, flattened double-walled carbon nanotubes (FDWCNTs) and epoxy are used as the inorganic and polymer components, respectively, to generate layered composites. The selection of two-dimensional (2D) FDWCNTs and epoxy was made on the following reasons: i) compared with traditional 1D cylindrical CNTs, FDWCNTs are more suitable as 2D fillers for bioinspired fabrication of the layered composites; ii) FDWCNTs show much better mechanical properties than typical 2D inorganic additives for mimicking nacre structures, such as glass flakes,[10] alumina flakes,[11] graphene oxide,[12] nanoclays,[13] and layered double hydroxides (LDHs);[14] and, iii) epoxy has wide application in daily life, including in high-strength plastic materials and general purpose adhesives. The experimental results confirm that the prepared composites show a hierarchical layered nano-/micro-structure, in which the CNTs are aligned and with a high loading amount of up to 70 wt%. Both the ultimate tensile strength and toughness of the FDWCNT-reinforced epoxy composites are remarkably higher than those of other reported CNT/epoxy composites.

Multi-layered FDWCNT films were first synthesized by a modified process reported previously.[15] In a furnace, the individual double-walled carbon nanotubes (DWCNTs) were spontaneously organized into a random multilayered film with a thickness of several hundred micrometers, called the FDWCNT film. The FDWCNT film was blown out with the carrier gas and then collected by the roller at the end of the quartz tube (Figure S1a in the Supporting Information). Figure S1b shows a photograph of an obtained freestanding FDWCNT film, which is flexible and can be easily folded into a desired shape without any damage (Figure S1c).

Scanning electron microscopy (SEM) reveals the multi-layered structure of the FDWCNT film (**Figure 1**a). Note that each freestanding layer inside the film has a thickness of several hundred nanometers (Figure 1b) and is composed of randomly entangled nanowires (Figure 1c). High-resolution transmission electron microscopy (HRTEM) (Figure 1d) further shows that every nanowire is a bundle consisted of many individual DWCNTs in the shape of a dog-bone;[16] these are stacked with each other through van der Waals force. Previous theoretical calculation and experimental results demonstrate that the hollow cylindrical DWCNTs with the diameters larger than a critical value of 4.96 nm[17] easily collapse and fold into flattened ribbons, because single DWCNTs have super-high stiffness and strength along their axial direction.[18] As shown in the right TEM image in Figure 1d, as-synthesized DWCNTs typically have diameters of 5.0–7.0 nm; thus, they spontaneously fold into ribbon-like FDWCNTs that subsequently aggregate to form the nanowires (left TEM image in Figure 1d). The structural characteristics of FDWCNTs are discerned by Raman spectroscopy (Figure S2) and thermogravimetric analysis (TGA) measurements, which further indicate that the content of FDWCNTs is approximate 82 wt% (Curve a in Figure S3). The residuals are most likely amorphous carbon and the iron catalysts. Before being used in the preparation of bioinspired layered composites, the synthesized FDWCNT films need purification (see the details in the Experimental Section). After purification, the content of FDWCNTs can reach 95 wt% (Curve b in Figure S3). All the above results are similar to those for previously obtained FDWCNT films.[15]

Dr. Q. F. Cheng, Prof. L. Jiang
Key Laboratory of Bio-inspired Smart Interfacial Science and Technology of Ministry of Education
School of Chemistry and Environment
BeiHang University
Beijing 100191, PR China
E-mail: cheng@buaa.edu.cn
Prof. Z. Y. Tang
National Center for Nanoscience and Technology
Beijing 100190, PR China
E-mail: zytang@nanoctr.cn
Dr. M. Z. Li
Institute of Chemistry
Chinese Academy of Sciences
Beijing 100190, PR China

DOI: 10.1002/adma.201200179

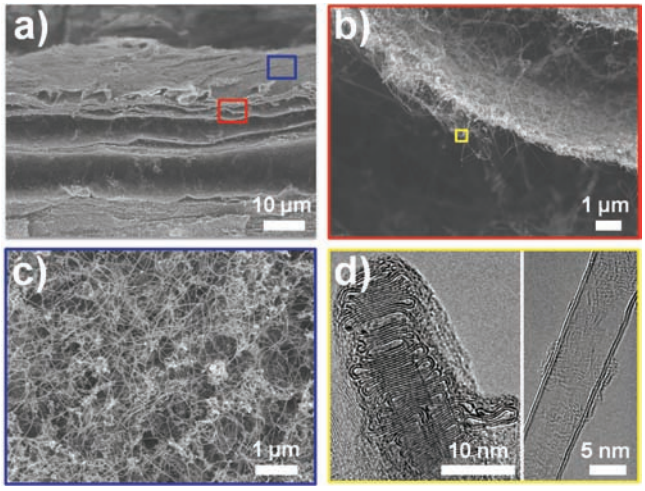

Figure 1. a) Cross-sectional SEM image of an FDWCNT film, showing its many layered structure. b) Magnified image of one layer of (a). c) Magnified top view of (a). d) Left: HRTEM image of single nanowires in (c); right: single DWCNT. The diameter of DWCNT is about 5.0–7.0 nm, which is larger than the critical value of 4.96 nm for formation of nanowires via self-folding.

Subsequently, bioinspired layered composites are fabricated following the procedure described in **Figure 2**a. The multi-layered FDWCNT films are aligned by mechanical stretching;[7] a cross-section of the FDWCNT film shows most nanowires consisted of DWCNTs bundles are well-aligned and stacked together along the direction of stretching (Figure 2c) compared with random DWCNTs bundles (Figure 2b). The alignment effect of FDWCNT can be characterized by polarized Raman spectroscopy, since the Raman intensity of the G-band vibration mode of CNTs is sensitive to its polarization angle.[19] The G-band peaks at different angles between the FDWCNT axis and the direction of laser polarization are shown in Figure S4a (see the Suporting Information). The G-band intensity reaches a maximum when the polarized light is parallel to the axes of nanotubes, and decreases gradually when the polarized light is switched to be perpendicular to the axes of nanotubes. The intensities are further normalized to the value at 0° and plotted as a function of π (Figure S4b). The degree of alignment is calculated to be about 0.8, according to a previous report,[7] which means that about 80% of FDWCNTs are probably aligned after stretching. Subsequently, the aligned FDWCNT films are treated with m-CPBA (m-chloroperoxybenzoic acid)/CH_2Cl_2 solution in order to graft the epoxide groups onto the surface of the FDWCNTs (Figure 2d).[20] Attenuated total reflectance Fourier transform infrared (ART-FTIR) spectroscopy demonstrates successful modification of epoxide-group on the FDWCNTs (Curve b in Figure S5). Finally, the epoxide-grafted FDWCNT films are impregnated with a solution of epoxy resin. After evaporation of the solvent, the composites are hot-pressed and cured into the layered film. In the process of epoxy curing, the functional groups of epoxide on the DWCNT surfaces react with epoxy constituents, resulting in cross-linking between FDWCNTs and epoxy matrix in chemical bonds (Figure 2e). Disappearance of epoxide-group peak of the functionalized FDWCNTs in the ATR-FTIR spectra confirms the occurrence of the cross-linking reaction (Curve c in Figure S5).

It is well known that the hierarchical structural features of natural nacre can be classified into two length scales: nanoscale and microscale.[9a] At the nanoscale (first level), aragonite nanograins with sizes of 10 –30 nm are glued together to form platelets with thicknesses of submicrometers.[21] At the microscale (second level), these platelets are staggered into a 3D brick-and-mortar structure that is enveloped by biopolymer.[9a,22] Analysis of the cross-section (**Figure 3**a) and surface (Figure 3b) of the aligned FDWCNT/epoxy composites indicates that the layered structure is maintained and the orientation of the aligned FDWCNTs is retained during the fabrication process. The first level in the structure of the composites is the nanowires, with diameters of about 10 nm; these consist of FDWCNT bundles, which are glued to form single layers (Figure 3c and d). At the second level, many layers of FDWCNT/epoxy are held together to

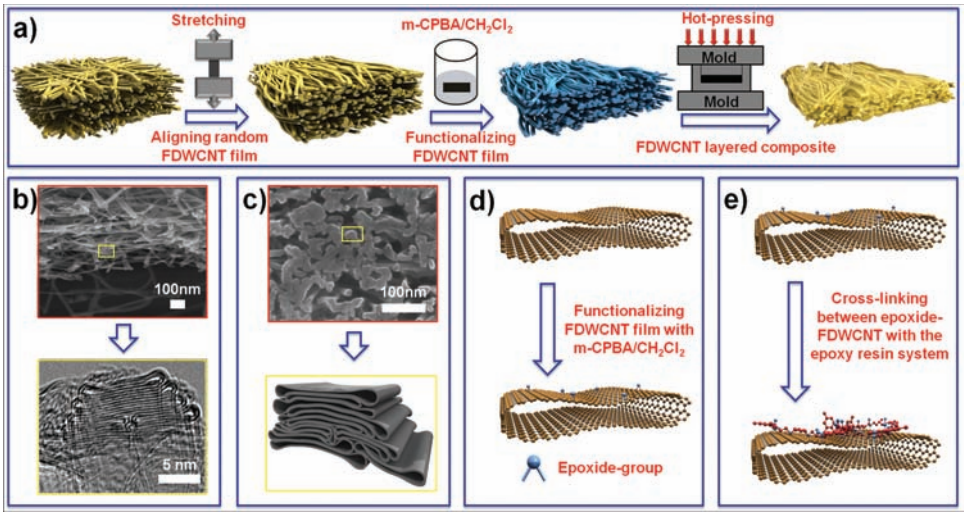

Figure 2. a) Scheme of fabrication of the bioinspired layered FDWCNT/epoxy composites. b) As-prepared FDWCNTs film. c) Cross-section of the aligned FDWCNT film. d) Introduction of epoxide groups on the FDWCNTs via treatment with m-CPBA/CH2Cl2. e) Cross-linking between FDWCNTs with epoxy matrix in chemical bonds.

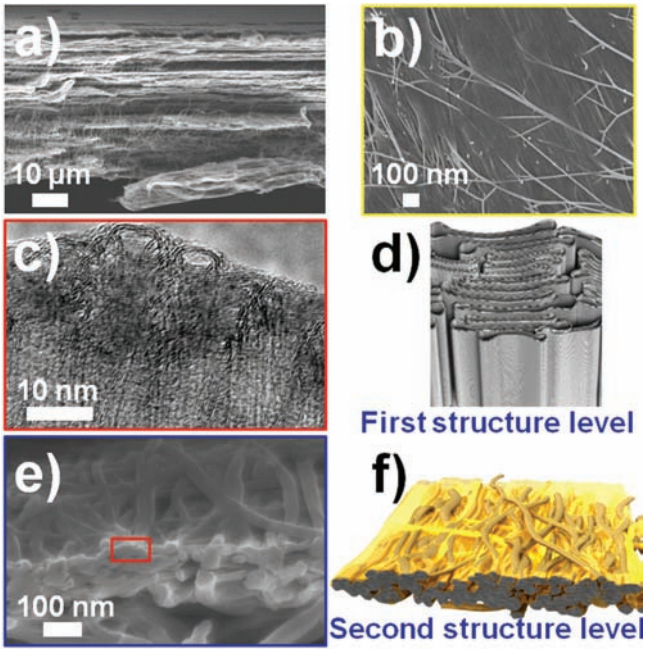

Figure 3. a) SEM image of the cross-section of the aligned FDWCNT/epoxy composites. b) SEM image of the surface of the aligned FDWCNTs/epoxy composites. c) TEM image of the cross-section of the nanowires composed of FDWCNT bundles, which represents the first level of the bioinspired layered composites. d) Cartoon of (c); several FDWCNTs are stacked together into the nanowires. e) One layer of the FDWCNT/epoxy film, representing the second structure level of the bioinspired layered composites. f) Cartoon of (e); yellow color represents the epoxy resin.

form thin-film composites, in which the thickness of each layer is around 100 nm (Figure 3e and f). Evidently, both the size of individual nanowire and the thickness of single FDWCNT layer are comparable to the structural features inside natural nacre.

Generally, the mechanical performance of hybrid organic–inorganic composites falls far below theoretical predictions suggest, due to three major problems: i) low volume fraction of inorganic reinforcement, ii) lack of structural control, and, iii) low effective load transfer.[13b] Especially for CNTs, because of their strong self-aggregation tendency, it is very difficult for the high CNT loading to be incorporated homogeneously into the polymer matrix. Inspired by the layered structures of natural nacre, several previous methods, such as layer-by-layer (LBL) assembly,[13a,b] paper making,[23] ice-templated fabrication,[24] and bottom-up colloidal assembly[25] have been successfully used to obtain high volume fraction of inorganic reinforcement. Herein, the bioinspired layered FDWCNT/epoxy composites have high loading amounts of FDWCNTs, at around 70 wt% (Figure S6 in the Supporting Information). This is possibly because, compared with conventional cylindrical CNTs, the flattened shape of FDWCNTs can occupy a higher fraction in the same area of composites (Figure S7). It should be pointed out that, different to many nacre-mimetic composites that are prepared by tedious multilayer deposition processes, the layered FDWCNT/epoxy composites are easily obtained and moreover the thickness of the layered FDWCNT/epoxy composites easily reaches that of bulk materials; thick FDWCNT-reinforced epoxy composites are critical for their practical application.

The other important factor to achieve good mechanical performance is the need for well-controlled structures at both nanoscale and macroscale in the artificial materials,[13b] for example the bioinspired layered composites are produced by applying 2D platelets including glass flake, alumina flake, graphene oxide and nanoclay, which have the layered feature. In order to construct well-ordered hierarchical structures based on FDWCNTs, random FDWCNT films are first aligned by mechanical stretching using a previously developed method.[7] As shown in Figure 2, the nanowires composed of FDWCNTs are well packed into one layer along the stretching direction. The functionalized FDWCNTs work as do the bricks inside nacre; the difference is that the FDWCNTs have much higher mechanical performance and are more flexible compared with other 2D platelets. Thus, a combination of high loading of ultrastrong FDWCNTs and the hierarchical nano-/micro-structures is expected to remarkably enhance the mechanical performance of epoxy-based composites.

The mechanical properties of the layered composites containing randomly-distributed FDWCNTs are first examined. Their ultimate tensile strength is measured to be 0.45 ± 0.03 GPa (Curve 2 in **Figure 4**a). Notably, the obtained tensile

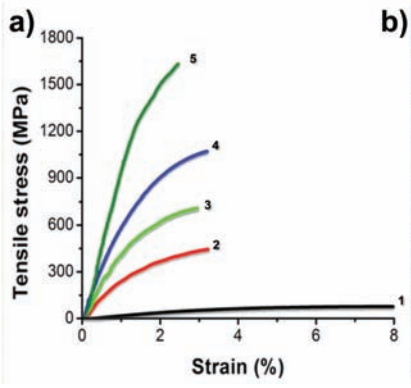

b)

Mechanical properties comparison of bioinspired layered composite with other CNT/epoxy composites					
Materials	**Strength, σ (MPa)**	**Modulus, E (GPa)**	**Toughness (MJ/m³)**	**CNT loading**	**Year Ref.**
SWCNT/epoxy fiber	900-1600	30-50	21.6	30-40 vol%	2009[3c]
SWCNT/epoxy fiber	253	18.8	1.9	27 vol%	2009[26]
3-D MWCNT/epoxy braid	314.8	23.9	2.5	40 vol%	2010[27]
Aligned MWCNT/epoxy	231.5	20.4	1.4	16.5 wt%	2010[8]
Aligned MWCNT/epoxy	402	22.3	6.8	32 wt%	2010[28]
Random FDWCNT/epoxy	450 ± 30	32 ± 2.0	9.6 ± 1.0	70 wt%	Our data
Random FDWCNT/epoxy with crosslinking	700 ± 20	56 ± 1.0	14.0 ± 1.3		
Aligned FDWCNT/epoxy	1070 ± 100	65 ± 5.0	23.2 ± 2.0		
Aligned FDWCNT/epoxy with crosslinking	1600 ± 200	107 ± 16.0	24.5 ± 1.5		

Figure 4. a) Tensile stress–strain curves of the bioinspired layered FDWCNT/epoxy composites: Curve 1 is the pure epoxy resin; Curve 2 represents the random FDWCNT/epoxy composites; Curve 3 is the random FDWCNT/epoxy composites after cross-linking; Curve 4 is the aligned FDWCNT/epoxy composites; and, Curve 5 represents the aligned FDWCNT/epoxy composites after cross-linking. b) Mechanical properties comparison between bioinspired layered composites with other CNT/epoxy composites.

strength is not only five times higher than that of neat epoxy resin (Curve 1 in Figure 4a), but also larger than the highest value of artificial nacre fabricated with montmorillonite (MTM) and poly(vinyl alcohol) (PVA) so far.[13b] On the other hand, the tensile strength and toughness of the layered random FDWCNT/epoxy composite have exceeded that of other multi-walled carbon nanotube (MWCNT) reinforced epoxy composites fabricated by infiltration,[26] 3D braiding,[27] resin-transfer molding,[8] and buckypaper.[28] This good mechanical performance of the layered random FDWCNT/epoxy composites should originate from the high volume fraction of FDWCNTs and the high friction between FDWCNTs due to their flattened shape and large surface contact.[29] More impressively, the mechanical properties of composites containing pre-aligned FDWCNTs can be further improved. The tensile strength increases from 0.45 ± 0.03 to 1.07 ± 0.10 GPa (Curve 4 in Figure 4a), while the Young's modulus increases from 32 ± 2.0 to 65 ± 5.0 GPa. The increase in the mechanical property of composites mainly results from improvement of the mechanical strength of neat FDWCNT films via alignment: the tensile strength increases from 135 ± 15 to 300 ± 25 MPa, while the Young's modulus increases from 0.70 ± 0.3 to 6.20 ± 1.2 GPa (Figure S8 in the Supporting Information). Moreover, the improvement in the load transfer efficiency from epoxy to the aligned FDWCNTs also corresponds to enhancement of the mechanical property of composites.

The interfacial interaction between organic and inorganic phases plays a key role in determining the mechanical properties of composites. Sliding between organic and inorganic phases frequently occurs in natural nacre when the loading force is greater than the interfacial interaction.[21,22,30] This phenomenon is also observed in the pull-out experiments of CNTs from polymer matrix.[31] Chemical cross-linking of organic and inorganic phases would increase the interfacial interaction and thus significantly improve the overall mechanical performance of composites as in the case of, for example, metal-infiltrated spider silk.[32] Herein, the covalent attachment of chemical groups is used to enhance the interfacial interaction between FDWCNTs and epoxy. Figure S9 illustrates the proposed cross-linking mechanism. The FDWCNTs are first functionalized with epoxide groups by peroxide acid m-CPBA (Step 1 in Figure S9). Then, the epoxide-FDWCNT are reacted with epoxy resin system (Steps 2–4 in Figure S9) so that a chemical bond of carbon–oxygen is formed between FDWCNTs and epoxy resin, which effectively enhance the load transfer efficiency from epoxy to FDWCNTs. For layered random FDWCNT/epoxy composites, the ultimate tensile strength increases to 0.70 ± 0.02 GPa, and Young's modulus increases to 56 ± 1.0 GPa, corresponding to 55% and 75% improvement, respectively (Curve 3 vs. Curve 2 in Figure 4a). For layered aligned FDWCNT/epoxy composites, the ultimate tensile strength reaches up to 1.60 ± 0.20 Gpa, and Young's modulus as high as 107 ± 16.0 GPa (Curve 5 in Figure 4a). It should be stressed that the maximum tensile strength of 1.8 GPa is comparable to super-tough CNT/PVA fibers,[3b] and obviously is higher than that of SWCNT/epoxy fibers,[3c] being twenty times higher than that of pure epoxy matrix (Curve 1 in Figure 4a). Moreover, the highest Young's modulus of the aligned FDWCNT/epoxy composites after cross-linking, 123 GPa, is sixty times higher than that of pure epoxy matrix and two times higher than the maximum stiffness of SWCNT/epoxy fibers.[3c]

Important parameters to evaluate the mechanical performance of the materials should include tensile strength, Young's modulus, and toughness. Figure 4b further summarizes the mechanical performance of the layered FDWCNT/epoxy composites and other reported CNTs/epoxy composites. Until now, the best mechanical performance of CNT/epoxy composites has been obtained with single-walled carbon nanotube (SWCNT) fiber reinforced epoxy composites;[3c] the maximum tensile strength, Young's modulus, and toughness reported are 1600 MPa, 50 GPa, and 21.6 MJ m^{-3}, respectively. As comparison, the maximum tensile strength, Young's modulus, and toughness of the layered aligned FDWCNT/epoxy composites via cross-linking are 1800 MPa, 123 GPa and 26.0 MJ m^{-3}, respectively. It is evident that the mechanical performance of the reported materials outperforms other existing materials.

In conclusion, the bioinspired layered FDWCNT reinforced epoxy composites are successfully fabricated. In comparison with previous methods, this bioinspired strategy has the following crucial advantages: i) it dramatically enhances the CNT loading in the composite products, ii) it generates CNT/epoxy composites with the layered hierarchical nano-/micro-structures, iii) it creates CNT/epoxy composites with high tensile strength, Young's modulus, and toughness, and, iv) it can quickly produce the layered composites in a large quantity. This study provides a novel route to produce high performance CNT-reinforced polymer composites, which will have great promising applications in research and industrial fields.[33]

Experimental Section

Materials: Flattened double-walled carbon nanotubes (FDWCNTs) were synthesized by following the modified process reported before.[15] FDWCNT films were continuously produced by the experimental set-up, which consisted of a quartz tube reactor in the centre of an electric furnace (Figure S1a). A mixture of alcohol and acetone (1:1 v/v) was used as the carbon source. Ferrocene dissolved in the carbon source was selected as catalyst. The thiophene was mixed with the precursors as a promoter. After ultrasonication for 10 min at room temperature, the mixed solution became transparent brown. Then the solution was injected into the quartz tube reactor via a syringe pump. The solvent injection rate was in the range of 20–60 mL h^{-1}. A mixture of argon and hydrogen (1:1 to 1:10 v/v) was used as the carrier and active gas, respectively, at the flow rate in the range of 800–3000 mL min^{-1}. The synthesis temperatures were controlled in the range 1000–1300 °C. The products were carried out from the hot zone of the furnace by the gas flow and spun into film at the end of the quartz tube.

Purification Process: As-grown FDWCNT film was first soaked into a 30% hydrogen peroxide solution for 72 h at 60 °C. Then, the FDWCNT film was transferred into a 37% hydrogen chloride solution for 12 h. Finally, the FDWCNT film was washed thoroughly by ultrapure water. After the purification, the combined content of amorphous carbon and iron catalyst were below 5%.

Aligning FDWCNT Film: The FDWCNT film was aligned by mechanical stretching according to our previous work.[7] The FDWCNT film was cut into rectangle strips, which were stretched by the mechanical machine with the speed of 0.5 mm min^{-1}. The stretching deformation was irreversible and retraction could not happen after stretching, because the aligned FDWCNTs in the film stacked each other with strong van der Waals forces.

Epoxidation Functionalization of FDWCNT Film: The random and aligned FDWCNT film was immersed in m-CPBA (m-chloroperoxybenzoic acid)/CH_2Cl_2 (dichloromethane) solution for 10 min, and then washed with dichloromethane to remove residual m-CPBA. The functionalized FDWCNT film was placed in a vacuum oven at 80 °C for 30 min to evaporate the residual dichloromethane.

Fabrication of Bioinspired Layered Composites: Both random and aligned FDWCNT films were used to fabricate the bioinspired layered composites. The epoxy resin matrix consisted of glycidyl ester (A), methyltetrahydrophthalic anhydride (MTHPA) as the curing agent (B), and benzyldimethylamine (BDMA) as accelerator (C). The epoxy resin, curing agent, and accelerator were mixed at a weight ratio A/B/C of 100:100:2. The epoxy resin system was supplied by Beijing Institute of Aeronautical Materials (BIAM), China. The mechanical properties of this type of epoxy resin were listed in Table S1 (see the Supporting Information). First, the FDWCNT film was impregnated with epoxy resin solution to prepare FDWCNT prepregs with approximately 70 wt% loading of CNTs. The concentration of epoxy resin in the solution was adjusted to ensure low viscosity for facilitating impregnation. The residual solvent (acetone) was removed under 80 °C in the vacuum oven for 2 h. Second, the FDWCNT prepreg was cured by the hot-press process at high pressure following the curing cycle: 80 °C for 2 h plus 120 °C for 12 h. The weight percentage of CNTs was determined by the weight of the total amount of FDWCNTs used during composite fabrication. The weight ratio of FDWCNTs in the final composite was measured by TGA to be about 70 wt%.

Characterization: The structure of FDWCNT film was characterized by field emission scanning electron microscopy (FESEM, JEOL JSM-6700, Japan) at 3 kV, and transmission electron microscopy (TEM, JEM-2100F, Japan). The FDWCNT films were easily peeled off and directly placed on copper grid for TEM observation. Raman analysis (Renishaw inVia, England) was conducted using an Ar laser (wavelength = 633 nm). Thermogravimetric analysis (PE, TGA-7, USA) was performed to evaluate the carbon yield in the products, which was conducted by heating the samples at 20 °C min^{-1} from room temperature to 1000 °C. Mechanical properties tests were conducted using an INSTRON 5848 MicroTester with a crosshead speed of 1 mm min^{-1} and a gauge length of 10 mm under room temperature.

Supporting Information

Supporting Information is available from the Wiley Online Library or from the author.

Acknowledgements

QFC and MZL contributed equally to this work. This work was supported by the National Research Fund for Fundamental Key Projects (2010CB934700, 2011CB935700, 2009CB930404, 2009CB930401, 2007CB936403), the Research Fund for the Doctoral Program of Higher Education (20101102120044), the National Natural Science Foundation (51103004, 21003132, 20920102036, 209774113, 91127038), the National Natural Science Foundation for Distinguished Youth Scholars of China (21025310), the 100-Talent Program of Chinese Academy of Sciences and the National Science Foundation of China (20973047), and the Scientific Research Foundation for the Returned Overseas Chinese Scholars, State Education Ministry, PR China.

Received: January 13, 2012
Published online: March 14, 2012

[1] a) M.-F. Yu, O. Lourie, M. J. Dyer, K. Moloni, T. F. Kelly, R. S. Ruoff, *Science* **2000**, *287*, 637; b) B. Peng, M. Locascio, P. Zapol, S. Li, S. L. Mielke, G. C. Schatz, H. D. Espinosa, *Nat. Nanotechnol.* **2008**, *3*, 626.
[2] P. M. Ajayan, J. M. Tour, *Nature* **2007**, *447*, 1066.
[3] a) B. Vigolo, A. Penicaud, C. Coulon, C. Sauder, R. Pailler, C. Journet, P. Bernier, P. Poulin, *Science* **2000**, *290*, 1331; b) A. B. Dalton, S. Collins, E. Munoz, J. M. Razal, V. H. Ebron, J. P. Ferraris, J. N. Coleman, B. G. Kim, R. H. Baughman, *Nature* **2003**, *423*, 703; c) W. Ma, L. Liu, Z. Zhang, R. Yang, G. Liu, T. Zhang, X. An, X. Yi, Y. Ren, Z. Niu, J. Li, H. Dong, W. Zhou, P. M. Ajayan, S. Xie, *Nano Lett.* **2009**, *9*, 2855; d) K. Liu, Y. H. Sun, X. Y. Lin, R. F. Zhou, J. P. Wang, S. S. Fan, K. L. Jiang, *ACS Nano* **2010**, *4*, 5827; e) D. Blond, W. Walshe, K. Young, F. M. Blighe, U. Khan, D. Almecija, L. Carpenter, J. McCauley, W. J. Blau, J. N. Coleman, *Adv. Funct. Mater.* **2008**, *18*, 2618; f) X. M. Sui, H. D. Wagner, *Nano Lett.* **2009**, *9*, 1423.
[4] Z. Wang, Z. Y. Liang, B. Wang, C. Zhang, L. Kramer, *Composites Part A* **2004**, *35*, 1225.
[5] B. L. Wardle, D. S. Saito, E. J. Garcia, A. J. Hart, R. G. de Villoria, E. A. Verploegen, *Adv. Mater.* **2008**, *20*, 2707.
[6] B. S. Shim, J. Zhu, E. Jan, K. Critchley, S. Ho, P. Podsiadlo, K. Sun, N. A. Kotov, *ACS Nano* **2009**, *3*, 1711.
[7] Q. F. Cheng, J. W. Bao, J. G. Park, Z. Y. Liang, C. Zhang, B. Wang, *Adv. Funct. Mater.* **2009**, *19*, 3219.
[8] Q. F. Cheng, J. P. Wang, J. J. Wen, C. H. Liu, K. L. Jiang, Q. Q. Li, S. S. Fan, *Carbon* **2010**, *48*, 260.
[9] a) H. D. Espinosa, J. E. Rim, F. Barthelat, M. J. Buehler, *Prog. Mater. Sci.* **2009**, *54*, 1059; b) H.-B. Yao, H.-Y. Fang, X.-H. Wang, S.-H. Yu, *Chem. Soc. Rev.* **2011**, *40*, 3764.
[10] H. Kakisawa, T. Sumitomo, R. Inoue, Y. Kagawa, *Compos. Sci. Technol.* **2010**, *70*, 161.
[11] a) O. Oner Ekiz, A. F. Dericioglu, H. Kakisawa, *Mater. Sci. Eng. C* **2009**, *29*, 2050; b) L. J. Bonderer, K. Feldman, L. J. Gauckler, *Compos. Sci. Technol.* **2010**, *70*, 1958.
[12] a) Y. Xu, W. Hong, H. Bai, C. Li, G. Shi, *Carbon* **2009**, *47*, 3538; b) K. W. Putz, O. C. Compton, M. J. Palmeri, S. T. Nguyen, L. C. Brinson, *Adv. Funct. Mater.* **2010**, *20*, 3322.
[13] a) Z. Tang, N. A. Kotov, S. Magonov, B. Ozturk, *Nat. Mater.* **2003**, *2*, 413; b) P. Podsiadlo, A. K. Kaushik, E. M. Arruda, A. M. Waas, B. S. Shim, J. D. Xu, H. Nandivada, B. G. Pumplin, J. Lahann, A. Ramamoorthy, N. A. Kotov, *Science* **2007**, *318*, 80; c) H. B. Yao, Z. H. Tan, H. Y. Fang, S. H. Yu, *Angew. Chem., Int. Ed.* **2010**, *49*, 10127.
[14] H. B. Yao, H. Y. Fang, Z. H. Tan, L. H. Wu, S. H. Yu, *Angew. Chem., Int. Ed.* **2010**, *49*, 2140.
[15] a) K. Koziol, J. Vilatela, A. Moisala, M. Motta, P. Cunniff, M. Sennett, A. Windle, *Science* **2007**, *318*, 1892; b) X. Zhong, Y. Li, Y. Liu, X. Qiao, Y. Feng, J. Liang, J. Jin, L. Zhu, F. Hou, J. Li, *Adv. Mater.* **2010**, *22*, 692.
[16] M. Motta, A. Moisala, I. A. Kinloch, H. W. Alan, *Adv. Mater.* **2007**, *19*, 3721.
[17] J. Xiao, B. Liu, Y. Huang, J. Zuo, K. C. Hwang, M. F. Yu, *Nanotechnology* **2007**, *18*.
[18] M. F. Yu, M. J. Dyer, R. S. Ruoff, *J. Appl. Phys.* **2001**, *89*, 4554.
[19] A. M. Rao, A. Jorio, M. A. Pimenta, M. S. S. Dantas, R. Saito, G. Dresselhaus, M. S. Dresselhaus, *Phys. Rev. Lett.* **2000**, *84*, 1820.
[20] D. Ogrin, J. Chattopadhyay, A. K. Sadana, W. E. Billups, A. R. Barron, *J. Am. Chem. Soc.* **2006**, *128*, 11322.
[21] F. Barthelat, C. M. Li, C. Comi, H. D. Espinosa, *J. Mater. Res.* **2006**, *21*, 1977.
[22] M. A. Meyers, P. Y. Chen, A. Y. M. Lin, Y. Seki, *Prog. Mater. Sci.* **2008**, *53*, 1.
[23] A. Walther, I. Bjurhager, J. M. Malho, J. Ruokolainen, L. Berglund, O. Ikkala, *Angew. Chem., Int. Ed.* **2010**, *49*, 6448.
[24] a) E. Munch, M. E. Launey, D. H. Alsem, E. Saiz, A. P. Tomsia, R. O. Ritchie, *Science* **2008**, *322*, 1516; b) S. Deville, E. Saiz, R. K. Nalla, A. P. Tomsia, *Science* **2006**, *311*, 515.
[25] A. R. Studart, L. J. Bonderer, L. J. Gauckler, *Science* **2008**, *319*, 1069.

[26] R. J. Mora, J. J. Vilatela, A. H. Windle, *Compos. Sci. Technol.* **2009**, *69*, 1558.
[27] A. E. Bogdanovich, P. D. Bradford, *Composites Part A* **2010**, *41*, 230.
[28] P. D. Bradford, X. Wang, H. Zhao, J.-P. Maria, Q. Jia, Y. T. Zhu, *Compos. Sci. Technol.* **2010**, *70*, 1980.
[29] X. Zhang, Q. Li, *ACS Nano* **2010**, *4*, 312.
[30] a) R. Z. Wang, Z. Suo, A. G. Evans, N. Yao, I. A. Aksay, *J. Mater. Res.* **2001**, *16*, 2485; b) F. Song, Y. Bai, *J. Mater. Res.* **2003**, *18*, 1741; c) B. Bruet, H. Qi, M. Boyce, R. Panas, K. Tai, L. Frick, C. Ortiz, *J. Mater. Res.* **2005**, *20*, 2400.
[31] A. H. Barber, S. R. Cohen, H. D. Wagner, *Phys. Rev. Lett.* **2004**, *92*, 186103.
[32] S. M. Lee, E. Pippel, U. Gosele, C. Dresbach, Y. Qin, C. V. Chandran, T. Brauniger, G. Hause, M. Knez, *Science* **2009**, *324*, 488.
[33] G. M. Luz, J. F. Mano, *Philos. Trans. R. Soc. London, Ser. A* **2009**, *367*, 1587.